

Improvement of Proton-Exchange Membranes Based on $(1 - x)(\text{H}_3\text{PO}_2/\text{PVA}) - x\text{TiO}_2$

M. E. Fernández ¹, G. Murillo Y. ² R. A. Vargas ³, D. Peña Lara ⁴ and J. E. Diosa ⁵

Received: 27-11-2016 | Accepted: 25-04-2017 | Online: 08-05-2017

MSC: 82D60 | PACS: 72.80.Le, 72.80.Tm, 66.30.hk, 66.30.jp

doi:10.17230/ingciencia.13.25.6

Abstract

Using impedance spectroscopy (IS), differential scanning calorimetry (DSC), thermogravimetric analysis (TGA), and infrared spectroscopy (IR) techniques to study the polymer electrolyte membranes based on poly(vinyl alcohol) (PVA) and hypophosphorous acid (H_3PO_2) with different titanium oxide nanoparticles (TiO_2) concentrations. The polymer systems $(1-x)(\text{H}_3\text{PO}_2/\text{PVA}) + x\text{TiO}_2$ were prepared using the sol-casting method and different weight percent of TiO_2 , $x \leq 10.0\%$. The DSC results show that the glass transition for molar fraction $\text{P}/\text{OH} = 0.3$ appears around

¹ Universidad del Valle, mariaferlo2000@yahoo.com,
<http://orcid.org/0000-0003-4228-9693>, Cali, Colombia.

² Universidad Icesi, gustavo.murillo@correo.icesi.edu.co,
<http://orcid.org/0000-0001-5172-4584>, Cali, Colombia.

³ Universidad del Valle, ruben.vargas@correounivalle.edu.co,
<http://orcid.org/0000-0002-2295-373X>, Cali, Colombia.

⁴ Universidad del Valle, diego.pena@correounivalle.edu.co,
<http://orcid.org/0000-0001-6199-1547>, Cali, Colombia.

⁵ Universidad del Valle, jesus.diosa@correounivalle.edu.co,
<http://orcid.org/0000-0002-1919-1922>, Cali, Colombia.

75°C and for the samples doped with TiO_2 around 35°C; the melting point for all membranes appear around 175°C. The FTIR spectra show changes in the profiles of the absorption bands with the addition of H_3PO_2 and the different concentrations of TiO_2 . The IS results show dielectric and conductivity relaxations as well as a change in DC ionic conductivity with the TiO_2 content. The order of the ionic conductivity is about 10^{-2} S/cm for 5.0% of TiO_2 . The TGA in the heating run shows water loss that is in agreement with DC conductivity measurements.

Key words: Composite polymer membranes; PVA; Hypophosphorous acid; Proton conduction, DC conductivity.

Mejoras en membranas de intercambio protónico $(1-x)(\text{H}_3\text{PO}_2/\text{PVA})-x\text{TiO}_2$

Resumen

Usando las técnicas de espectroscopia de impedancia (IS), calorimetría de barrido diferencial (DSC), análisis termogravimétrico (TGA) y espectroscopia infrarroja (FTIR) se estudió el sistema polimérico $(1-x)(\text{H}_3\text{PO}_2/\text{PVA}) + x\text{TiO}_2$ el cual fue preparado usando el método de *sol-casting* a diferentes porcentaje de peso de nanopartículas de TiO_2 , $x \leq 10.0\%$. Los resultados de DSC muestran que la transición vítrea para la fracción molar de $\text{P}/\text{OH} = 0.3$ emerge alrededor de 75°C y para las muestras dopadas con TiO_2 alrededor de 35°C; el punto de fusión para todas las membranas aparece alrededor de los 175°C. Los espectros de FTIR muestran cambios en los perfiles de las bandas de absorción con la adición del H_3PO_2 y las diferentes concentraciones de TiO_2 . Los resultados de IS muestran relajaciones dieléctricas y de conductividad al igual que un cambio en la conductividad iónica DC con el contenido de TiO_2 . La conductividad iónica es del orden de 10^{-2} S/cm para 5.0% de TiO_2 . Los TGA en los barridos de calentamiento muestran pérdida de agua lo cual está de acuerdo con las medidas de conductividad DC.

Palabras clave: Membranas poliméricas compositos; PVA; conducción protónica.

1 introduction

The Proton Exchange Membranes (PEMs) are the most promising for Fuel Cells (FC) technologies to generate clean energy [1],[2],[3],[4]. Perfluorinated Nafion[®] is the most used membrane for FC applications [5],[6],

due to excellent chemical stability and a marked effect on the proton conductivity. A more economical alternative for preparing PEM was proposed in 1989 [7] which is a combination of poly(vinyl alcohol) (PVA) and hypophosphorous acid. This new combination allowed the production of non-perfluorinated membranes of low cost and good procesability, encouraging manufacturing different types of PEMs, which have been synthesized using mixtures of polymers with various salts and acids [8]. Other groups have investigated various combinations using PVA as polymeric matrix [8],[9],[10],[11],[12]. On the other hand, composites have been synthesized based on polymeric membranes combined with micro or nanoparticles for the purpose of controlling the physical and chemical properties, being in some cases that this approach has improved proton conductivity and mechanical properties for some dispersant concentrations [13],[14],[15],[16]. In this work the polymer membrane ($\text{H}_3\text{PO}_2/\text{PVA}$) with constant molar ratio $\text{P}/\text{OH} = 0.3$, doped with TiO_2 nanoparticles have been synthesized and studied its effect on the thermal and electrical properties.

2 Experimental methods

The precursors materials were hypophosphorous acid (H_3PO_2), PVA, and titanium oxide (TiO_2) with particle size smaller than 50 nm (Sigma Aldrich Chemicals). PVA was poured in distilled water at 90°C using a magnetic stirrer plate to completely dissolve the polymer. After turning off the stirrer, constant amounts of acid were added to the solution, according to the molar ratio $\text{P}/\text{OH} = 0.3$. Then, constant amounts of TiO_2 nanoparticles were added to the solution, maintaining the mixture under agitation until it became homogeneous. After additional two hours under agitation the mixture, now at room temperature, was poured into glass vessels under dry atmosphere (desiccator with sulphuric acid) by several days to obtain membranes. The resulting membranes were uniform, smooth, homogeneous with a constant white color on the whole surface due to the presence of highly dispersed TiO_2 nanoparticles, and having a thickness of 0.2 mm.

The thermal characterization was carried out by using a TA Instrument DSC Q100 calorimeter at a thermal scan of $10^\circ\text{C}/\text{min}$ under a nitrogen atmosphere in a temperature range between -75°C and 250°C . Thermogravimetric characterization (TG) was carried out with a TA instruments 2050

TGA microbalance at a temperature rate of $10^\circ\text{C}/\text{min}$ under a nitrogen atmosphere from ambient temperature to 180°C .

The electrical characterizations of the samples were performed by impedance spectroscopy (IS) using an Agilent 4294A impedance analyzer in a frequency range 40 Hz to 6 MHz, with a voltage signal of 500 mV peak-to-peak. The measurements were done at isotherms separated by 10°C between room temperature and 120°C , under an air atmosphere. Cylindrical silver electrodes of 5.0 mm in diameter were used to contact the samples. The dc conductivity was determined from the bulk sample resistance using the impedance plots, Z , by extrapolation of the circular portion of the spectrum to the real axis Z' , and then using the expression $\sigma_0 = d/AR$ being R the intercept with the Z' -axis, d the membrane thickness, and A the sample contact area with the electrodes. The Jonscher model [17]

$$\sigma(\omega) = \sigma_0 + A\omega^n \quad (1)$$

was used to determine σ_0 by fitting experimental data, where σ_0 is the dc conductivity (independent of frequency), A is a pre-exponential factor related to crossover frequency, ω_p , and n is between 0 and 1.

From the impedance data, $Z'(\omega)$ and $Z''(\omega)$, the values for real part of the conductivity (σ'), real part (ϵ'), and imaginary part (ϵ'') of the permittivity were obtained by following relations:

$$\sigma'(\omega) = \frac{Z''}{Z'^2 + Z''^2} \quad (2)$$

$$\epsilon' = \frac{Z''}{\omega C_0(Z'^2 + Z''^2)} \quad (3)$$

$$\epsilon'' = \frac{Z'}{\omega C_0(Z'^2 + Z''^2)} \quad (4)$$

where C_0 is the empty cell capacitance.

The Fourier transform infrared spectra, FT-IR, were recorded using a Vertex 70 with resolution 4 cm^{-1} , on an interval from 4000 cm^{-1} to 500 cm^{-1} . Spectra were obtained at room temperature and under a nitrogen atmosphere.

3 Result and discussions

Typical DSC curves for $(1 - x)(\text{H}_3\text{PO}_2/\text{PVA}) - x\text{TiO}_2$ membranes with constant ratio $\text{P}/\text{OH} = 0.3$ and different concentrations x (for 0.0%, red; 2.5%, green; 5.0%, blue; 7.5%, navy; 10.0%, olive) of TiO_2 are depicted in Figure 1.

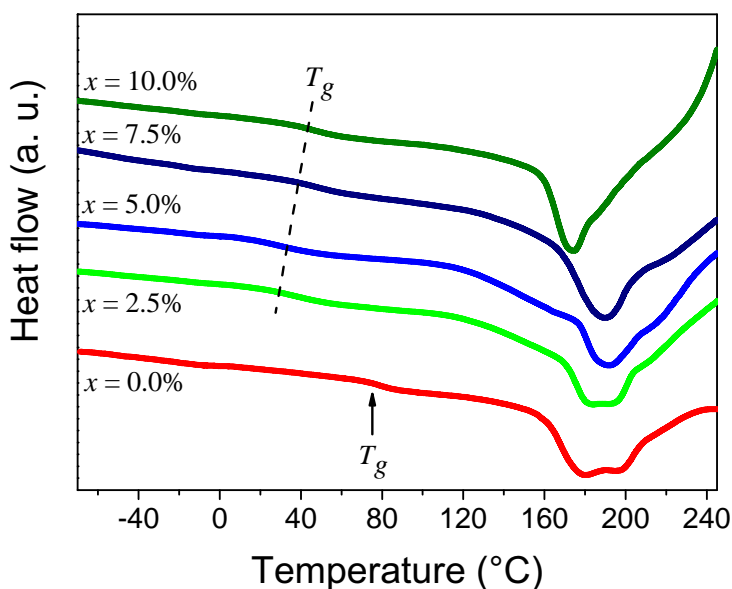


Figure 1: DSC curves for the $(1 - x)(\text{H}_3\text{PO}_2/\text{PVA}) - x\text{TiO}_2$ membranes with TiO_2 content of $x = 0.0\%$ (red), 2.5% (green), 5.0% (blue), 7.5% (navy), and 10.0% (olive), from -75°C to 250°C using a heating rate of $10^\circ\text{C}/\text{min}$ under a dry N_2 flux. The vertical arrow (for $x = 0.0\%$) and the dotted line (for $x = 2.5\%$, 5.0%, 7.5%, and 10.0%) indicate T_g .

It was reported [8] previously, for H_3PO_2 and PVA based membranes with acid high concentrations and high degree of hydration of the polymer that the glass transition temperature (T_g) was below 0.0°C . In our case, for low acid concentrations ($\text{P}/\text{OH} = 0.3$, $x = 0.0\%$) the T_g is around 75°C (as indicated by the vertical arrow) while for TiO_2 doped samples the T_g

appears around 35°C (as indicated by a dotted line), thus clearly indicating the effect of the oxide filler. The melting point for all membranes is observed at around 175°C .

FT-IR spectra for PVA and $(1-x)(\text{H}_3\text{PO}_2/\text{PVA})-x\text{TiO}_2$ system are showed in Figure 2.

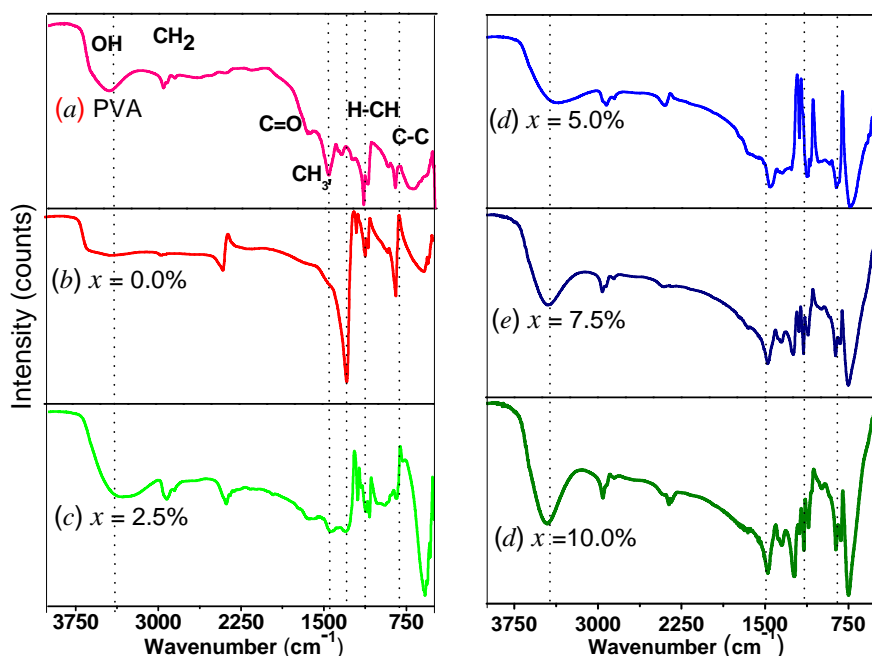


Figure 2: FT-IR spectra of PVA and $(1-x)(\text{H}_3\text{PO}_2/\text{PVA})-x\text{TiO}_2$ with TiO_2 content of $x = 0.0\%$ (red), 2.5% (green), 5.0% (blue), 7.5% (navy), and 10.0% (olive).

For pure PVA, four characteristic absorption bands are observed: the one at 3485 cm^{-1} which is assigned to vibration along the C–OH-chains bonds in PVA; the second one at 2957 cm^{-1} attributed to asymmetric elongation of the CH–CH₂-groups. The third one at 1477 cm^{-1} was associated with CH-cross deformations in CH₂-groups and the fourth band at 742 cm^{-1} was assigned to H–C–C–H-bound modes in the CH₂ groups. Additionally, the $\text{H}_3\text{PO}_2/\text{PVA}$ system was also characterized. In this case, two

additional bands appeared which were associated with vibration along the $V_{as}(PO_2)$ -antisymmetric bonds and the $V_s(PO_2)$ -symmetric bonds at 1269 cm^{-1} and 1102 cm^{-1} , respectively. Finally, by the addition of different TiO_2 concentrations, spectra show changes (movement and intensification of the peaks) for bands associated to CH_3 , PO_2 , CH_2 , and C–C functional groups. These changes might be related to effects of approximation of the nanoparticles with the polymer chains.

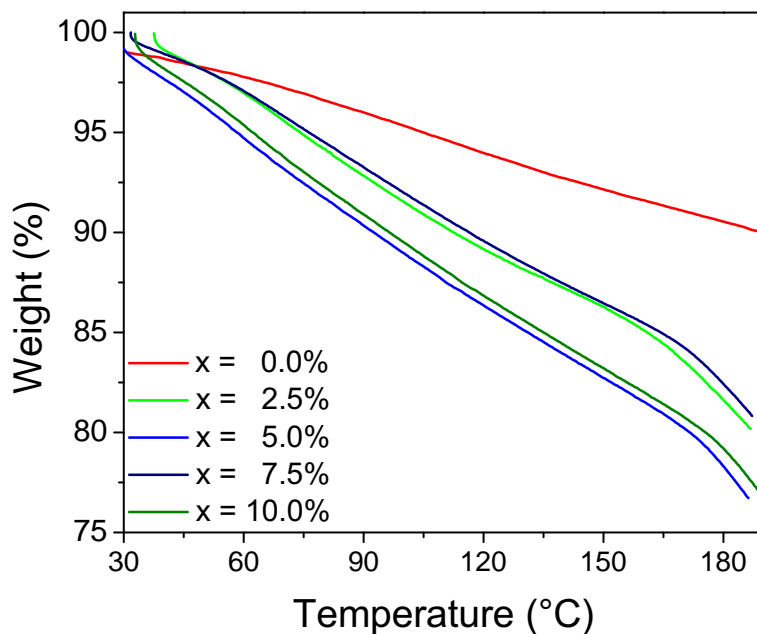


Figure 3: TGA curves of $(1 - x)(H_3PO_2/PVA) - xTiO_2$ with TiO_2 content of $x = 0.0\%$ (red), 2.5% (green), 5.0% (blue), 7.5% (navy), and 10.0% (olive).

Figure 3 shows the TGA curves of the membranes at a heating rate of $10^\circ\text{C}/\text{min}$. It is observed that all the TGA curves show a continuous weight loss as the temperature is increased. This loss is attributable to the evaporation of water molecules absorbed on the membrane surface or trapped within the chains of the polymer matrix. However, it is important to note that the losses presented between room temperature and 100°C increases with the concentration of TiO_2 indicating higher water content

in the fresh samples as the oxide filler content increases. Later on, the electrical measurements will reflect the influence of water removal from the samples on their proton conductivities.

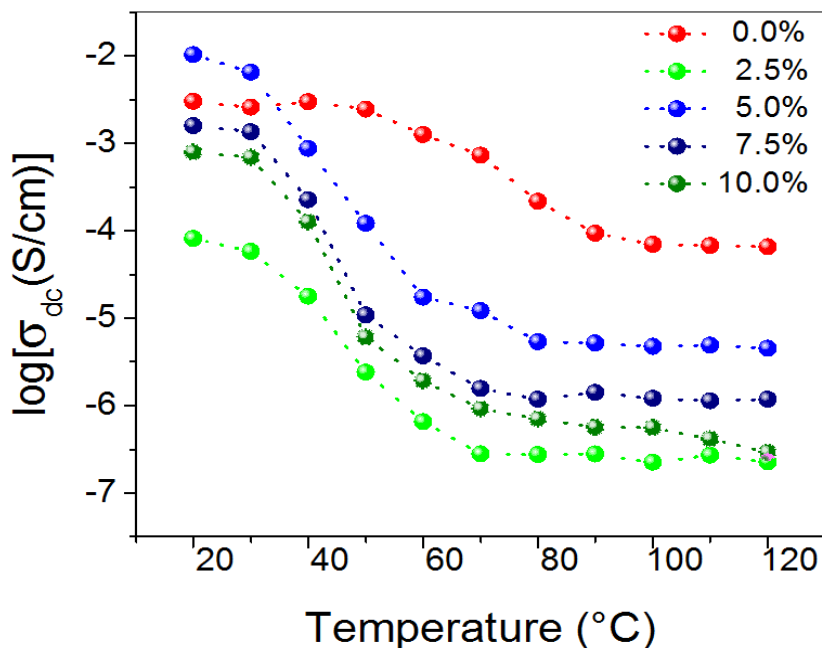


Figure 4: Temperature variation of the dc conductivity of $(1-x)(\text{H}_3\text{PO}_2/\text{PVA})-x\text{TiO}_2$ with TiO_2 content of $x = 0.0\%$ (red), 2.5% (green), 5.0% (blue), 7.5% (navy), and 10.0% (olive).

Figure 4 shows the temperature variation of dc conductivity on a logarithm scale calculated from the impedance Nyquist plots of the $(1-x)(\text{H}_3\text{PO}_2/\text{PVA})-x\text{TiO}_2$ membrane. The results show that dc conductivity values decrease with increasing temperature in the range where the membranes release water as noted in the results of TGA (see Figure 3) indicating that the proton transport membranes is provided in regions containing water that form a liquid phase or aqueous solution with H_3PO_2 . This liquid phase coexists with a solid phase of the reinforced polymer, consisting of PVA, the acid which is not dissolved in the liquid phase, and the dispersed TiO_2 particles, as discussed in references [9] and [18] for similar

polymeric membranes. This phenomenon is common in perfluorinated hydrated membranes (Nafion[®]). The dc conductivity is between 10^{-5} S/cm to 10^{-2} S/cm at room temperature, being about 10^{-2} S/cm for 5.0% TiO₂. Furthermore, above a decreasing step of dc conductivity, it remains at a constant value with increasing temperatures for each concentration. Conductivity values in this high-temperature interval have values from 10^{-6} S/cm to 10^{-4} S/cm that depends on concentration and the highest one correspond to $x = 0.0\%$.

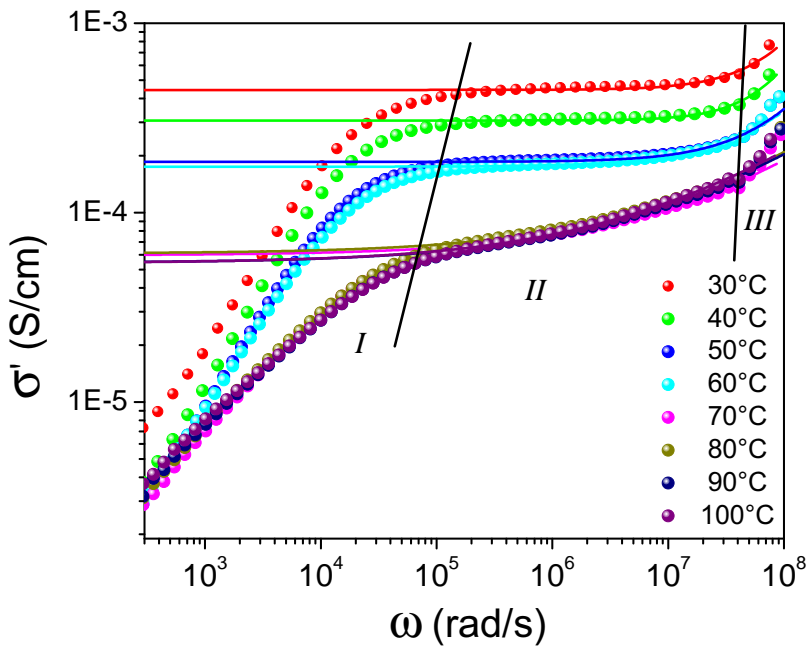


Figure 5: Log-log plot of the real part of the conductivity (σ') as a function of (angular) frequency (ω) for $(1-x)(\text{H}_3\text{PO}_2/\text{PVA})-x\text{TiO}_2$ with TiO₂ content of $x = 10.0\%$ at several isotherms at 30°C (red), 40°C (green), 50°C (blue), 60°C (cyan), 70°C (magenta), 80°C (dark yellow), 90°C (navy), and 100°C (purple). Solid line represents a Jonscher model fitting according to Equation (1).

Figure 5 shows the real part of the electrical conductivity σ' as a function of the (angular) frequency [$\omega = 2\pi f$ (Hz)] in double logarithmic scale at different isotherms. In all spectra it can be seen three distinct regions

as the temperature increases: at low frequency, a strongly dispersive initial region (*I*) which corresponds to the charge transfer processes at the electrode-electrolyte interface, followed by an intermediate less dispersive frequency region (*II*) corresponding to the long range ionic transport (dc-regime). Notice that σ' decreases with increasing temperature between 20°C and 120°C. Finally, a highly dispersive frequency region (*III*), in which the conductivity increases rapidly with increasing frequency. This phenomenology can be attributed to strong correlations in the hopping of charge carriers (relaxation of conductivity). The behavior in region *II* and *III* follow the power law proposed by Jonscher [17], $\sigma'(\omega) = \sigma_0 + A\omega^n$, where n is a fractional exponent between 0 and 1. The parameter n has been proposed to be close to 1 for strongly correlated ion motion and to be equal to zero for completely random and independent Debye-like ion hops [17]. The Jonscher phenomenological model was used to fit the experimental data of the conductivity σ' as a function of frequency represented by a solid line in Figure 5 to obtain σ_0 , n , and ω_p parameters.

Table 1: Fitting parameters obtained from the Jonscher model for membrane with concentration $x = 10.0\%$.

T (°C)	n	A	σ_0 (S/cm)
30	1.23	4.620×10^{-14}	4.44×10^{-4}
40	1.44	8.298×10^{-16}	3.06×10^{-4}
50	1.00	1.253×10^{-12}	1.85×10^{-4}
60	0.86	2.048×10^{-11}	1.74×10^{-4}
70	0.46	2.939×10^{-8}	5.95×10^{-5}
80	0.44	4.134×10^{-8}	6.08×10^{-5}
90	0.43	5.879×10^{-8}	5.43×10^{-5}
100	0.42	6.411×10^{-8}	5.42×10^{-5}

Table 1 gives the values for n , A , and σ_0 according to Jonscher model for the membrane with $x = 10.0\%$. It is important to stress that the dc conductivity (σ_0) values coincide those calculated from Nyquist plots. On the other hand, the n -exponent parameters are between 0 and 1, except data recorded at 30°C and 40°C which give values higher than 1 that may be associated with high values of energy storage in the collective movements of the short-range ions and which can not be explained by Jonscher

model. Moreover, the crossover frequency (ω_p) values decrease with increasing temperature similar to those of dc conductivity. This observation indicates that all processes of ion transport, either long-range (dc conductivity) or relaxation (characterized by the frequency ω_p), have the same origin, that is, migration (jump) of the charge carriers in the polymeric matrix.

In terms of the dielectric permittivity, calculated from equation (3) and (4) for its real and imaginary parts, we have:

$$\varepsilon(\omega) = \varepsilon'(\omega) - i\varepsilon''(\omega) \quad (5)$$

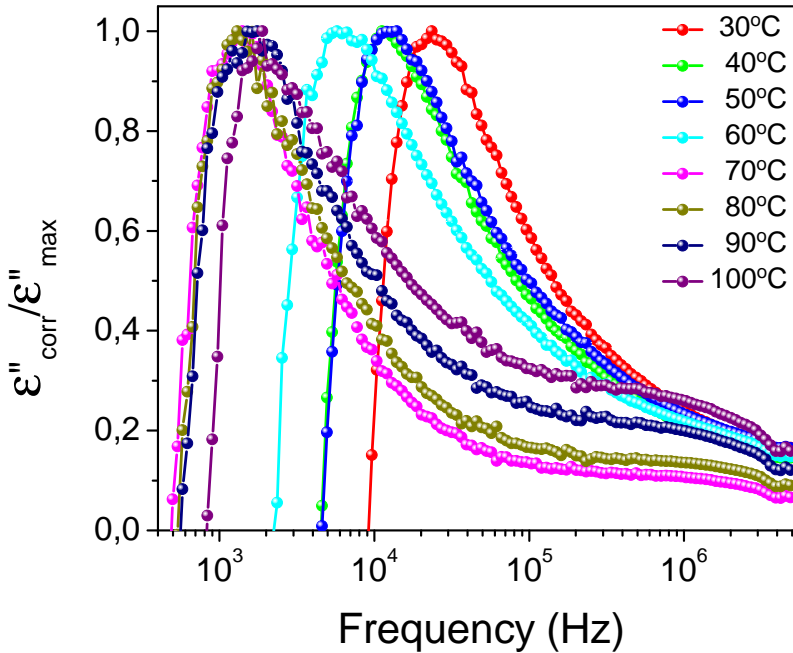


Figure 6: The corrected and normalized imaginary part of dielectric permittivity, $\varepsilon''_{\text{corr}}/\varepsilon''_{\text{max}}$, for the $(1-x)(\text{H}_3\text{PO}_2/\text{PVA})-x\text{TiO}_2$ membrane with TiO_2 content of $x = 10.0\%$ at different isotherms as a function of frequency in logarithm scale. The solid lines are guides to the eye.

Figure 6 shows the result for the corrected and normalized imaginary part of dielectric permittivity, $\varepsilon''_{\text{corr}}/\varepsilon''_{\text{max}}$, where $\varepsilon''_{\text{corr}} = \varepsilon'' - \sigma_0/w$ for the

composite concentration $x = 10.0\%$. Here we observe a dielectric relaxation peak at low temperature and relatively low frequency. This peak is observed at around 10^3 Hz at different isotherms. We attribute this relaxation to the presence of water in the polymer that introduce polar effect in the composite.

4 Conclusions

Composite polymer electrolyte based on PVA- H_3PO_2 , with constant molar ratio $\text{P}/\text{OH} = 0.3$, and reinforced with nanoparticles TiO_2 (doping concentration $x \leq 10.0\%$), homogenously dispersed, have been prepared. The TGA results show that the oxide filler of TiO_2 nanoparticles increases the water content in the hydrated composites. Moreover, the DSC results show that the glass transition for membranes based on H_3PO_2 and PVA with high acid concentrations and high degree of hydration of PVA is below 0°C , as reported previously, which is shifted to about 75°C for membranes with a low acid concentration of $\text{P}/\text{OH} = 0.3$, thus indicating that the acid aqueous solution plasticizes the polymer. However, when the membranes are reinforced with TiO_2 the glass transition temperature decrease to 35°C , thus suggesting that the water content increases due to the presence of the porous TiO_2 nanoparticles which increases the plasticity of the blends. On the other hand, the melting point appears at around 175°C for all membranes, close to that of the polymer matrix of PVA, indicating identical bond strength. Infrared spectroscopy spectra for pure PVA, as well as with acid content and with dispersed TiO_2 nanoparticles show variation in the absorption peaks indicating that the acid and TiO_2 are chemically coordinated to the PVA chains.

DC conductivity is in the range 10^{-5} S/cm to 10^{-2} S/cm at room temperature for TiO_2 concentrations examined, reaching its maximum value of 10^{-2} S/cm for a 5.0%- TiO_2 concentration.

The real part of the conductivity as a function of frequency shows a behavior known as Jonscher's power-law, with a crossover frequency (ω_p) associated with relaxation in the mobile ions. The temperature-dependency of ω_p follows the temperature variation of the dc conductivity, suggesting a common origin in these processes as a consequence of correlations among ions hopping.

The permittivity of the hydrated samples (at lower temperatures) shows as a function of frequency dielectric relaxation peaks in its imaginary part that we attribute to the polar effect of the water molecule in the membranes.

Acknowledgments

Financial support by Excellence Center for Novel Materials (CENM) is gratefully acknowledged.

References

- [1] B. Smitha, S. Sridhar, and A. Khan, "Solid polymer electrolyte membranes for fuel cell applications –a review," *J. Membrane Science*, vol. 259, pp. 10–26, 2005. 154
- [2] J. Rao and K. Geckeler, "Polymer nanoparticles: Preparation techniques and size-control parameters," *Progress in Polymer Science*, vol. 48, pp. 887–913, 2003. 154
- [3] H. Zhang and S. P. Kang, "Recent Development of Polymer Electrolyte Membranes for Fuel Cells," *Chem. Rev.*, vol. 112, pp. 2780–2832, 2012. 154
- [4] A. Mazuera and R. Vargas, "Electrical Properties and Phase Behavior of Proton Conducting Nanocomposites Based on the Polymer System $(1-x)[\text{PVOH} + \text{H}_3\text{PO}_2 + \text{H}_2\text{O}]\hat{\text{A}}x(\text{Nb}_2\text{O}_5)$," *Am. J. Analytical Chem.*, vol. 5, pp. 301–307, 2014. 154
- [5] J. B. Goodenough, "Proton conductors: Solids, membranes, and gels—materials and devices. edited by phillippe colomban, cambridge university press, cambridge, uk 1992, £ 75, xxxii, 581 pp., hardcover, isbn 0-521-38317-x," *Advanced Materials*, vol. 5, no. 9, pp. 683–685, 1993. [Online]. Available: <http://dx.doi.org/10.1002/adma.19930050923> 154
- [6] S. Banerjee and D. Curtin, "Nafion[®] perfluorinated membranes in fuel cells," *J. Fluorine Chem.*, vol. 125, pp. 1211–1216, 2004. 154
- [7] K. Gong and H. Shou-Cai, "Electrical Properties of Poly(Vinyl Alcohol) Complexed with Phosphoric Acid," *Mater. Res. Soc. Symp. Proc.*, vol. 135, pp. 377–382, 1989. 155
- [8] M. Vargas, R. Vargas, and B.-E. Mellander, "More studies on the PVAI+H₃PO₂ + H₂O proton conductor gels," *Electrochimical Acta*, vol. 45, pp. 1399–1403, 2000. 155, 157

- [9] I. Palacio, R. Castillo, and R. Vargas, "Thermal and transport properties of the polymer electrolyte based on poly (vinyl alcohol) –KOH–H₂O," *Electrochemical Acta*, vol. 48, pp. 2195–2199, 2003. 155, 160
- [10] V. Zapata, W. Castro, R. Vargas, and B.-E. Mellander, "More studies on the PVOH–LiH₂PO₄ polymer system," *Electrochimical Acta*, vol. 53, pp. 1476–1480, 2007. 155
- [11] W. Castro, V. Zapata, R. Vargas, and B.-E. Mellander, "Electrical conductivity relaxation in PVOH–LiClO₄–Al₂O₃," *Electrochimica Acta*, vol. 53, pp. 1422–1426, 2007. 155
- [12] M. Fernández, J. Castillo, F. Bedoya, J. Diosa, and R. Vargas, "Dependence of the mechanical and electrical properties on the acid content in PVA + H₃PO₂ + H₂O membranes," *Rev. Mex. Física*, vol. 60, pp. 249–252, 2014. 155
- [13] C. Yang, "Synthesis and characterization of the cross-linked PVA/TiO₂ composite polymer membrane for alkaline DMFC," *Electrochimical Acta*, vol. 288, pp. 51–60, 2007. 155
- [14] M. Fernández, J. Diosa, R. Vargas, J. Guerra, C. Villaquiran, D. García, and J. Eiras, "Influence of TiO₂ Nanoparticles on the Morphological, Thermal and Solution Properties of PVA/TiO₂ Nanocomposite Membranes," *Phys. Stat. Sol. (c)*, vol. 4, pp. 4075–4080, 2007. 155
- [15] P. Ahmadpoor, A. Nateri, and V. Motaghitalab, "The Optical Properties of PVA/TiO₂ Composite Nanofibers," *J. Applied Polymer Science*, vol. 130, pp. 78–85, 2013. 155
- [16] J. Ahmad, K. Deshmukh, M. Habib, and M. Hägg, "Influence of TiO₂ Nanoparticles on the Morphological, Thermal and Solution Properties of PVA/TiO₂ Nanocomposite Membranes," *J. Sci. Eng.*, vol. 39, pp. 6805–6814, 2014. 155
- [17] A. Jonscher, *Universal relaxation law: a sequel to Dielectric relaxation in solids*. Chelsea Dielectrics Press, 1996. 156, 162
- [18] G. Casalbore-Miceli, M. Yang, M. Camaioni, C.-M. Mari, Y. Li, M. Sun, and H. Ling, "Investigations on the ion transport mechanism in conducting polymer films," *Sol. Stat. Ionics*, vol. 131, pp. 6805–6814, 2000. 160